ARL-TR-7364 ● AUG 2015

US Army Research Laboratory

Development and Verification of Sputtered Thin-Film Nickel-Titanium (NiTi) Shape Memory Alloy (SMA)

by Cory R Knick and Christopher J Morris

NOTICES

Disclaimers

ARL-TR-7364 ● AUG 2015

US Army Research Laboratory

Development and Verification of Sputtered Thin-Film Nickel-Titanium (NiTi) Shape Memory Alloy (SMA)

by Cory R Knick and Christopher J Morris
Sensors and Electron Devices Directorate, ARL

REPORT DOCUMENTATION PAGE	*Form Approved* *OMB No. 0704-0188*

1. REPORT DATE *(DD-MM-YYYY)*	**2. REPORT TYPE**	**3. DATES COVERED (From - To)**
Aug 2015	Final	09/2014 to 05/2015

4. TITLE AND SUBTITLE	
Development and Verification of Sputtered Thin-Film Nickel-Titanium (NiTi) Shape Memory Alloy (SMA)	**5a. CONTRACT NUMBER**
	5b. GRANT NUMBER
	5c. PROGRAM ELEMENT NUMBER
6. AUTHOR(S)	**5d. PROJECT NUMBER**
Cory R Knick and Christopher J Morris	**5e. TASK NUMBER**
	5f. WORK UNIT NUMBER
7. PERFORMING ORGANIZATION NAME(S) AND ADDRESS(ES)	**8. PERFORMING ORGANIZATION REPORT NUMBER**
US Army Research Laboratory ATTN: RDRL-SER-L 2800 Powder Mill Road Adelphi, MD 20783-1138	ARL-TR-7364
9. SPONSORING/MONITORING AGENCY NAME(S) AND ADDRESS(ES)	**10. SPONSOR/MONITOR'S ACRONYM(S)**
	11. SPONSOR/MONITOR'S REPORT NUMBER(S)

12. DISTRIBUTION/AVAILABILITY STATEMENT

Approved for public release; distribution unlimited.

13. SUPPLEMENTARY NOTES

14. ABSTRACT

This report details the development of a co-sputtering process to yield a shape memory alloy (SMA) film with a controllable composition of nickel-titanium ($Ni_{50}Ti_{50}$) and transformation temperature around 60 °C. Shape memory effects were characterized using differential scanning calorimetry (DSC), for which we demonstrated martensite-austenite phase change at 57 °C for 1–3 µm films annealed at 600 °C for 1 h. We used wafer stress versus temperature measurements as additional confirmation for the repeatable measurement of reversible phase transformation peaking at 73 °C upon heating. Up to 62 MPa was available for actuation during the thermally induced phase change. Future work will involve fabricating functional microelectromechanical system (MEMS) devices (i.e., cantilevers, actuators, etc.) based on our $Ni_{50}Ti_{50}$ SMA.

15. SUBJECT TERMS

MEMS, microelectromechanical system, shape memory alloy, SMA, thermal actuation, sputtering, thin film

16. SECURITY CLASSIFICATION OF:			**17. LIMITATION OF ABSTRACT**	**18. NUMBER OF PAGES**	**19a. NAME OF RESPONSIBLE PERSON**
					Cory R Knick
a. REPORT	**b. ABSTRACT**	**c. THIS PAGE**			**19b. TELEPHONE NUMBER (Include area code)**
Unclassified	Unclassified	Unclassified	UU	16	301-394-1147

Standard Form 298 (Rev. 8/98)
Prescribed by ANSI Std. Z39.18

Contents

List of Figures

List of Tables

1. Introduction

Thin-film shape memory alloys (SMAs) based on nickel-titanium (NiTi) can be patterned into micron-sized structures based on standard lithography and microelectromechanical system (MEMS) processing and have already become a primary actuating mechanism in MEMS devices since the work output per volume of thin-film SMAs surpasses that of electrostatic, magnetic, bi-metallic, piezoelectric, and thermo-pneumatic actuators.[1] While the study of thin-film SMA materials is fairly well documented,[2–14] it was necessary for us to develop a process in-house to reliably produce these films so that we can ultimately make useful MEMS devices based on SMA actuators.

In this report, we discuss our development of a co-sputtering process to produce thin-film NiTi-based SMAs. We begin by reporting on the sputtering process parameters used and the resulting SMA thin-film characterization by energy dispersive spectroscopy (EDX), differential scanning calorimetry (DSC), and wafer stress versus temperature methods. Ultimately, we were successful in developing and demonstrating a repeatable method for producing NiTi thin films with phase transformation above ambient, in the 60–70 °C range. Going forward, this allows us the ability to create MEMS processes and devices integrated with our in-house NiTi actuator material.

2. Methods

2.1 Characterization of NiTi Material Properties

NiTi and nickel-titanium-copper (NiTiCu) films were co-sputtered using an AJA ATC 2200 co-sputter tool, with independent DC power supplies to 2 (or 3) different 4-inch targets. The targets used were a $Ni_{50}Ti_{50}$ target and a pure Ti target. For the NiTiCu alloy, an additional Cu target was used. Substrate rotation was used to obtain optimal uniformity and argon (Ar) pressure was controlled between 2–10 mTorr. These films were characterized using multiple techniques, including electrical resistivity measurements on a 280SI Sheet 4-point Resistivity Measurement System to quantify film uniformity across a 4-inch wafer. We performed the EDX film composition analysis using a Hitachi S-4500 scanning electron microscope (SEM) equipped with a PRISM[60] Princeton Gamma Tech detector using a beam acceleration voltage of 20 kV.

DSC was performed on a Perkin Elmer machine using a heating/cooling rate of 40 °C/min for the in-situ anneal scan and 3 °C/min to test for phase transformation temperatures in the SMA films. For DSC, the films were sputtered onto a sacrificial photoresist layer, released in acetone, and then rinsed with deionized water (DI) and dried before loading into DSC sample pans. The mass of each sample was recorded before and after the DSC run to verify adequate drying.

Stress versus temperature measurements were performed using a Toho FLX-2320-S wafer bow tool with controlled heating and cooling from 0 to 100 °C with a heating and cooling rate of 3 °C/min. For these experiments, we prepared 1- and 2-μm films of $Ni_{50}Ti_{50}$ by sputtering onto 4-inch silicon (Si) wafers and vacuum annealing at 600 °C for 1 h to crystallize the material. Wafer bow was measured experimentally from 0 to 100 °C at 3 °C/min heating/cooling rate, which allowed us to calculate and plot the temperature-dependent residual stress in the NiTi film for each wafer sample.

3. Results and Discussion

3.1 Sputtering Process Development

Ten different sputter recipes were carried out in the AJA, and the resulting films were analyzed in order to finally establish our goal of obtaining an equiatomic alloy of NiTi, which exhibited the shape memory effect. By keeping the 375-W DC power supplied to the NiTi target constant, we achieved an equiatomic composition by supplying an additional 250 W DC to a separate Ti target. The sputter recipes and resulting film compositions that we measured using EDX are listed in Table 1. Film thickness measurements at multiple locations in addition to post-sputter resistivity measurements indicated that film uniformity was very good, typically better than 8% non-uniformity across a 4-inch wafer based on 25 measured resistivity values, giving us confidence that the film composition is uniform across a 4-inch wafer. Of the 10 process recipes presented in Table 1, only Process 4 (the equiatomic $Ni_{50}Ti_{50}$ alloy) exhibited the shape memory effect above room temperature, as confirmed with DSC and temperature-dependent residual stress measurements.

Table 1 Sputtering recipes and EDX atomic composition characterization for NiTi and NiTiCu alloys

	Target Power (W)			
Process	NiTi	Ti	Cu	EDX
1	375	30	--	$Ti_{40}Ni_{60}$
2	375	60	--	$Ti_{42}Ni_{58}$
3	375	150	--	$Ti_{45}Ni_{55}$
4	**375**	**250**	**--**	$\mathbf{Ti_{50}Ni_{50}}$
5	375	300	--	$Ti_{53}Ni_{47}$
6	300	375	--	$Ti_{57}Ni_{43}$
7	375	300	50	$Ti_{52}Ni_{46}Cu_2$
8	375	300	75	$Ti_{52}Ni_{40}Cu_8$
9	375	300	100	$Ti_{52}Ni_{36}Cu_{12}$
10	375	300	125	$Ti_{52}Ni_{32}Cu_{16}$

3.2 Differential Scanning Calorimetry

DSC is widely used in the SMA literature to determine phase transformation temperatures for crystallized samples of thin-film material. The reversible shape memory effect is clearly demonstrated when an endothermic reaction takes place upon heating (martensite to austenite transformation), followed by the reverse (austenite to martensite) exothermic reaction upon cooling from high temperature. We performed a series of DSC scans to show crystallization of each alloy composition from Table 1, indicated by the large exothermic reaction at 468 °C in Fig. 1. We performed this anneal scan for each of the compositions in Table 1 and determined that all films crystallized below 500 °C.

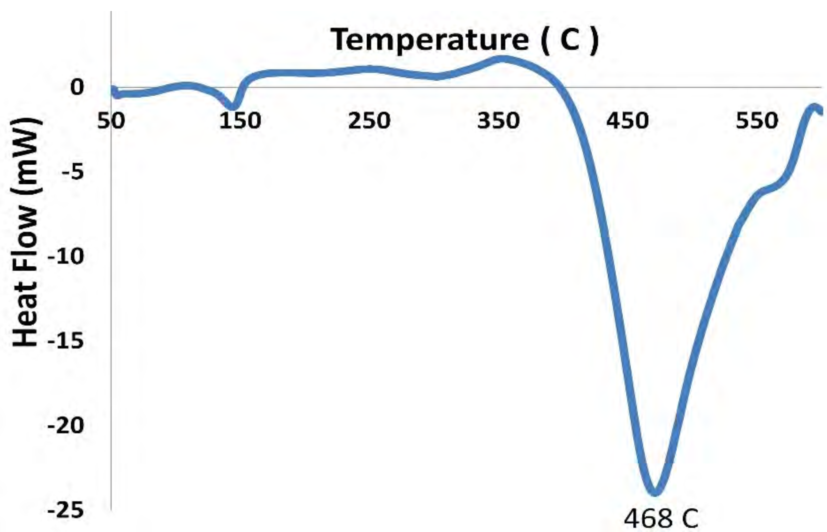

Fig. 1 In-situ anneal DSC curve for $Ni_{50}Ti_{50}$ showing crystallization of the amorphous film at 468 °C

To test for a shape memory effect in each composition, we performed a 3 °C/min scan from 35 to 100 °C, looking for an endothermic reaction on heating and an exothermic reaction upon cooling. The sample mass that we used was 5 mg at minimum, and up to 16 mg samples were tested. Samples of each composition listed in Table 1 were prepared by sputtering onto photoresist and lifting off the NiTi in acetone. Fig. 2 shows a DSC scan for the equiatomic $Ni_{50}Ti_{50}$. Of the compositions listed in Table 1, only the equiatomic NiTi recipe exhibited the shape memory effect when measured with DSC. The heating scan at 3° C/min shows the martensite to austenite peak phase transformation at 58 °C. The cooling scan shows the reverse austenite to martensite peak transformation at 55 °C. The reversible phase change was not detected above ambient for the other compositions, which is generally expected for off-equiatomic NiTi, especially in Ni-rich cases, where phase change has been reported as low as –100 °C. This is a good opportunity for us to note the sensitivity of phase change temperature to NiTi composition and stress the importance of achieving a uniform and repeatable equiatomic composition of NiTi, especially when phase change above room temperature is desired. Our achievement of a repeatable $Ni_{50}Ti_{50}$ thin-film composition with phase transformation temperature between 50 and 60 °C is a vital first step in realizing reliable MEMS actuators based on sputtered thin-film NiTi.

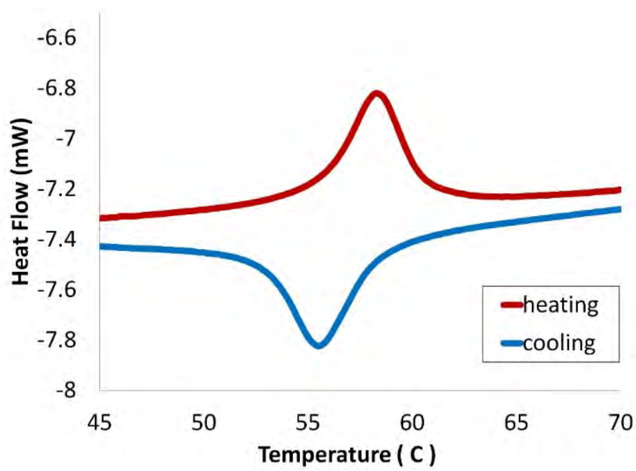

Fig. 2 DSC curve for 2-μm sputtered $Ni_{50}Ti_{50}$ annealed to 600 °C

3.3 Stress vs. Temperature Measurements

A useful and supplemental method for demonstrating the shape memory effect for films confined to a substrate is by the stress versus temperature method. This method is particularly important for us, because we can use the stress values as model input parameters to predict the folding radius of cantilever actuators whose actuation is dependent on the difference in residual stress in the 2 phases. We performed our scans with a heating/cooling rate of 3 °C/min to test for shape memory effect. Figure 3 shows a repeatable and reversible phase change with onset at 60 °C upon heating for 4 different wafers of $Ni_{50}Ti_{50}$. The maximum residual stress values peaked at 73 °C for each wafer in this experiment, indicated by the red curve during heating. An additional batch of NiTiCu wafers (Process 7–10 in Table 1) was measured using the same method, but the shape memory effect was not apparent, likely because the 600 °C rapid thermal anneal (RTA) used was not sufficient to generate the necessary shape memory effect. The stress versus temperature plots for NiTiCu alloys are shown in Fig. 4, even though the shape memory effect was not apparent. The off-equiatomic compositions of NiTi were not subjected to these measurements since a phase change above room temperature was not confirmed with DSC.

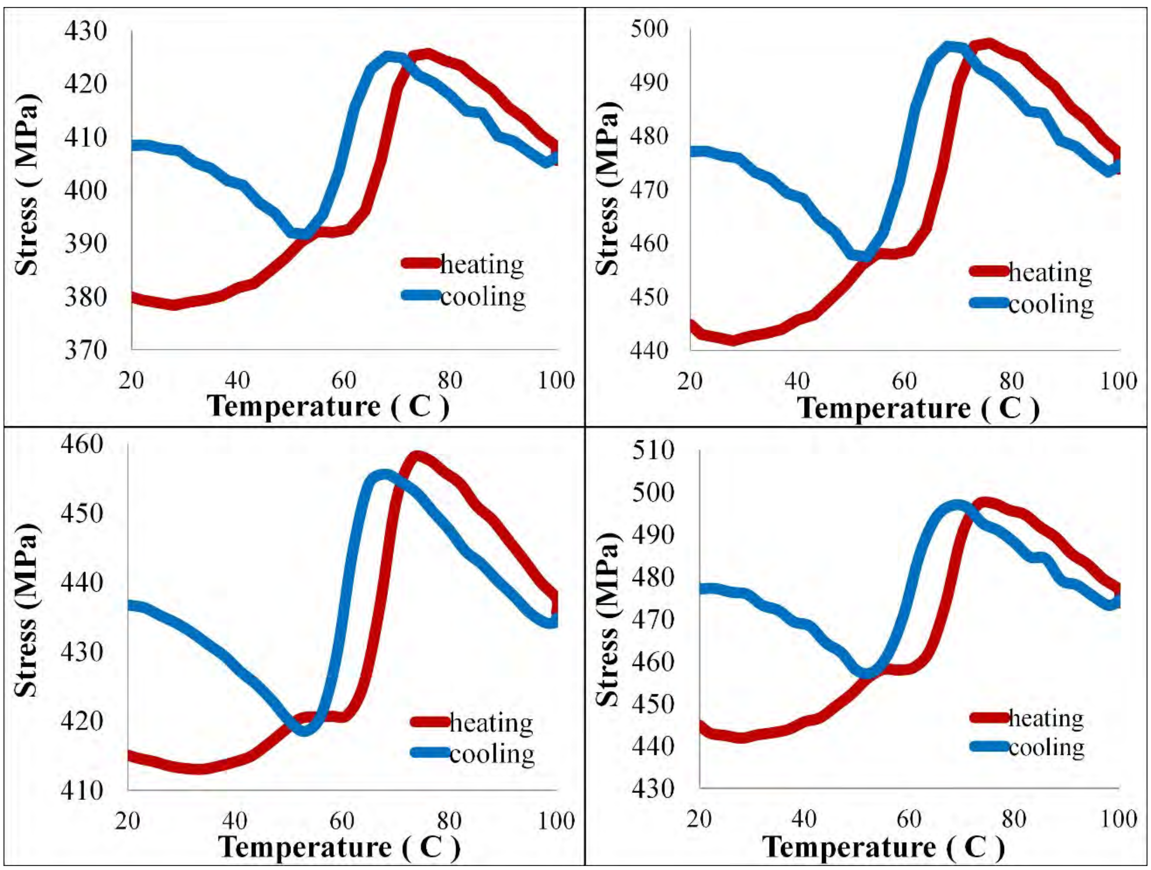

Fig. 3 **Stress vs. temperature measurements for 1- and 2-μm films of NiTi on a Si wafer**

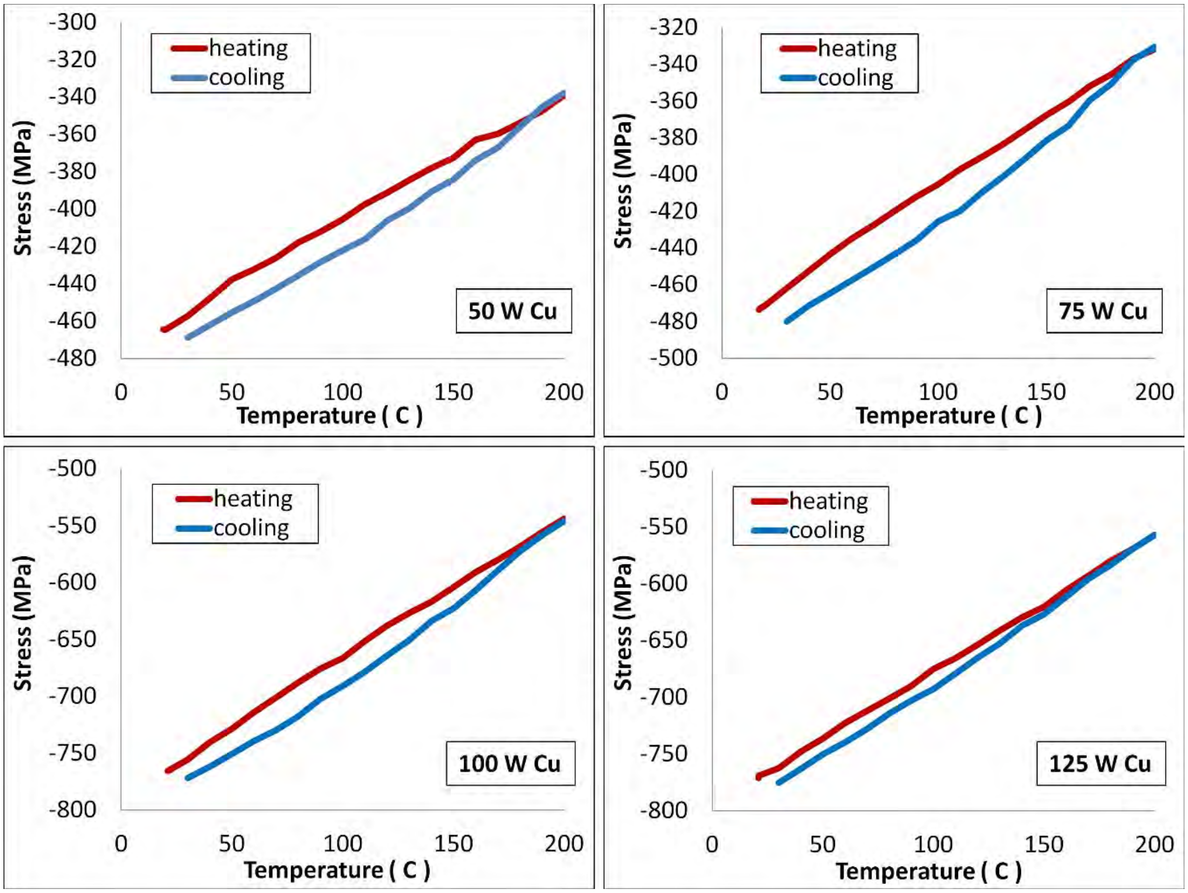

Fig. 4 Stress vs. temperature measurements for NiTiCu on a Si wafer

The NiTi residual stress in the martensite and austenite phases are shown in Table 2, as well as their difference, Δσ. Austenite phase stress was taken as the maximum stress value in the heating curve of the stress versus temperature plots, which reached a maximum at 73 °C in each case. We note that this measurement resolution was limited to 3 °C, corresponding to the heating and sampling rates used. This transition was recorded a few degrees higher than the DSC experiments. Previous work has reported stress changes from 50 to 500 MPa, but the films in our study appear to have too much residual stress in the initial martensite phase. It may be possible to tune the Ar gas pressure during the sputter process to get lower-stress films in the martensite phase, but that is the subject of future work. With the stress versus temperature results in Table 2 and Fig. 3, up to 62 MPa appears to be available for actuation.

Table 2 **NiTi thickness and residual stress in martensite and austenite phases**

		Stress σ (MPa)		
Wafer #	**NiTi thickness (um)**	**Martensite**	**Austenite**	**Δσ (MPa)**
1	1.10	380	430	50
2	0.90	320	345	25
3	0.95	445	500	55
4	2.10	340	363	23
5	2.30	330	392	62
6	2.00	415	458	43

4. Conclusions

We have shown that NiTi SMA material composition can be tuned by adjusting target power during a co-sputter process in order to create a $Ni_{50}Ti_{50}$ alloy composition exhibiting a shape memory effect in films as thin as 1 µm. We characterized 10 compositions of sputtered NiTi and NiTiCu thin films using DSC, EDX, and wafer stress versus temperature measurements, ultimately achieving an SMA material with a phase change temperature above ambient, near 60 °C with general repeatability. This was a vital step in order to realize a thermally actuated device in future work.

Future work will include decreasing the residual stress in the room temperature phase NiTi material. A byproduct of this achievement will be obtaining a larger stress differential between the 2 phases, thereby increasing the amount of useful work available from thermal actuation. Now that we have developed a reliable in-house sputtering process to create functional thin-film NiTi material, our next approach will be to integrate our material into functional devices (i.e., actuators, switches, etc.) using standard MEMS processing techniques.

5. References

1. Fu Y, Du H, Huang W, Zhang S, Hu M. TiNi-based thin films in MEMS applications: a review. Sens. Actuators A. 2004;112(2–3):395.
2. Hashinaga T, Miyazaki S, Ueki T, Horikawa H. J. Phys. 1995;IV:C8-689.
3. Kajiwara S, Yamazaki K, Ogawa K, Kikuchi T, Miyazaki S. Trans. Mater. Res. Soc. Jpn. 2001;26:183–188.
4. Chang L, Grummon DS. Philos. Mag. A. 1997;76:163–189.
5. Chang L, Grummon DS. Philos. Mag. A. 1997;76:191–219.
6. Winzek B, Quandt E. Metallkd. 1999;90:796–802.
7. Ren MH, Wang L, Xu D, Cai BC. Materi. Des. 2000;21:583–586.
8. Chu JP, Lai YW, Lin TN, Wang SF. Mater. Sci. Eng. A. 2000;277:11–17.
9. Chen JZ, Wu SK. J. Non-Cryst. Solids. 2001;288:271.
10. Craciunescu CM, Li J, Wutting M. Thin Solid Films. 2003;434:271.
11. Du H, Fu Y. Surf. Coat. Technol. 2004;176:182–187.
12. Quan J, Shan F, Wang W, Wang Y, Li M, Jin W. J. Mater. Sci. Lett. 2000;19:143–145.
13. Ishida A, Sato M, Ogawa K, Yamada K. Shape memory behavior of Ti-Ni-Cu thin films. Mater. Sci. and Eng. A. 2006;438–440:683–686.
14. Gill J, Ho K, Carman G. Three-dimensional thin-film shape memory alloy microactuator with two-way effect. J. Microelectromech. Sys. 2002;11:68–77.

List of Symbols, Abbreviations, and Acronyms

Ar	argon
Cu	copper
DI	deionized water
DSC	differential scanning calorimetry
EDX	energy dispersive spectroscopy
MEMS	microelectromechanical system
Ni	nickel
NiTi	nickel-titanium
NiTiCu	nickel-titanium-copper
RTA	rapid thermal anneal
SEM	scanning electron microscope
Si	silicon
SMAs	shape memory alloys
Ti	titanium

1 (PDF)	DEFENSE TECHNICAL INFORMATION CTR DTIC OCA
2 (PDF)	DIRECTOR US ARMY RSRCH LAB RDRL CIO LL IMAL HRA RECORDS MGMT
1 (PDF)	GOVT PRNTG OFC A MALHOTRA
3 (PDF)	DIRECTOR US ARMY RSRCH LAB RDRL SER L C KNICK C MORRIS B PIEKARSKI